

# Laser phase noise effects in fiber-optic signal processors with recirculating loops

M. Tur and B. Moslehi

Stanford University, Stanford, California 94305

Received December 14, 1982

The power spectrum of the optical intensity at the output of a single-mode-fiber recirculating delay line driven by a multimode semiconductor laser is shown to exhibit a spectral structure with notches at zero frequency as well as at other multiples of  $1/(\text{loop delay})$ . A theoretical model based on laser phase noise is suggested to explain the experimental data.

Recently, several fiber-optic signal processors were introduced that employ recirculating single-mode loops. These include the fiber-optic systolic matrix-vector multiplier<sup>1</sup> and the recirculating delay-line filter.<sup>2</sup> Proper operation of these processors requires the addition of optical intensities rather than amplitudes, and therefore short coherence sources must be used with a coherence time  $\tau_c$  much shorter than the smallest loop delay  $\tau$ . We demonstrate in this Letter that the dynamic range of the recirculating delay-line filter is severely limited by intensity noise whose origin is the laser phase fluctuations. We also show that the power spectrum of the output noise is characterized by minima at zero frequency as well as at other integer multiples of the inverse of the loop delay. Thus the spectral structure of this noise is entirely different from that of similarly originated noise, which occurs in nonrecirculating interferometric sensors<sup>3</sup> as well as in homodyne and heterodyne communication systems.<sup>4</sup> The power spectrum of the latter noise has its maximum at zero frequency,  $f = 0$ , and, when  $\tau_c$  is much smaller than the device delay  $\tau$ , the spectrum near  $f = 0$  is relatively flat within several  $1/\tau$  units.<sup>5</sup>

Figure 1 describes the experimental setup. As shown, the mechanically polished evanescent-field coupler<sup>6</sup> closes the delay line with no splices. The loop length was 27 cm, which corresponds to a delay of  $\tau = 1.35$  nsec. The continuous-wave GaAlAs multimode laser (General Optronics Model GO-ANA) runs with no external modulation. The  $P-I-N$  photodetector is followed by a 1–1000-MHz amplifier whose output is fed directly to the input of the spectrum analyzer. Curve A of Fig. 2 describes the spectrum of the amplifier output when the laser is off. Curve B shows the output spectrum when the coupler is disassembled into its two halves so that the laser light goes directly from the laser through the fiber into the detector. This spectrum is therefore characteristic of the intensity noise of the laser. Curve C was taken with an assembled coupler and a power-coupling ratio of approximately 40%. Here we see a much stronger spectrum with two notches (within the 1–1000-MHz range): one at  $f = 0$  and the other at a frequency of  $1/\tau$  ( $= 740$  MHz). Therefore the dynamic range of the loop, when the loop is operating as a filter, is limited not by the laser intensity noise but by a 20-dB stronger noise whose origin will be shown to be the laser

phase noise. The observed noise spectrum was found to be highly dependent on the coupling ratio. In particular, when this ratio was either 0 or 100%, the noise reduced to the level of curve B of Fig. 2, and a coupling ratio of 40% was found to give the highest noise. Figure 3 shows the spectrum for a 10-m loop ( $\tau = 50$  nsec) along with the intensity impulse response of the recirculating delay line [Fig. 3(b) was obtained by pulsing the laser with a single 35-nsec pulse]. Again, the spectrum is characterized by multiple notches equally spaced by  $1/\tau$ . In this longer loop it was possible to incorporate a manually adjustable polarization controller, which can change the state of polarization of the propagating wave without altering its degree of polarization.<sup>7</sup> As the state of polarization of the recirculating waves was varied, we observed up-and-down vertical shifts of a few decibels in the noise power spectrum, and Fig. 3 was obtained after the polarization controller was optimized to give maximum noise. Note that this spectral picture is

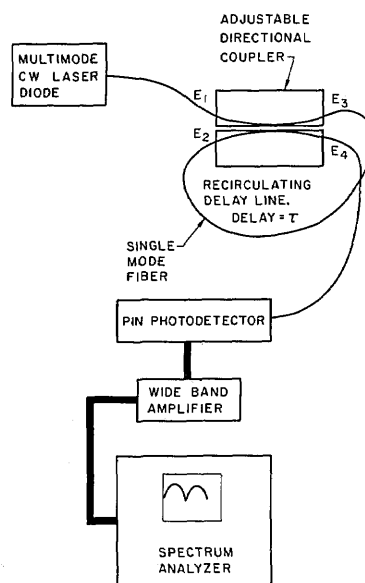


Fig. 1. Experimental setup for the measurement of the spectrum of the intensity noise at the output of a recirculating delay line, driven by a semiconductor laser.  $E_1$ ,  $E_2$  and  $E_3$ ,  $E_4$  are, respectively, the input and output fields. The optical power at the detector was  $130 \mu\text{W}$ , the loop length was 27 cm, and the amplifier gain was  $\approx 40$  dB.

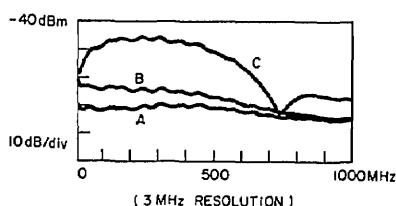


Fig. 2. Experimental noise spectra: A, the amplifier noise with the laser off; B, the laser intensity noise (the coupler is disassembled), and C, phase-induced noise with an assembled coupler (see Fig. 1).

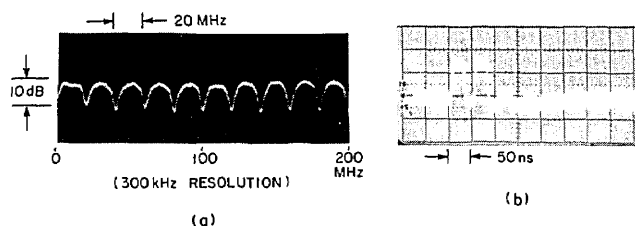


Fig. 3. A recirculating delay line with a 10-m loop. (a) Spectrum of the output intensity noise. The loop delay is 50 nsec, and the frequency spacing between successive notches is 20 MHz. (b) Intensity impulse response of the 10-m loop as determined by pulsing the laser with a 35-nsec pulse. The input pulse is partially coupled out (the first pulse in the picture); after one circulation it is split again, and the second pulse in the picture represents its uncoupled part. The process repeats itself, and this time-domain display clearly shows several recirculations.

complementary to the transfer function of the recirculating delay line when it is operating as a filter for rf modulation signals applied to the incident light.<sup>2</sup> It was experimentally determined that the above spectral structure was completely insensitive to loop-length variations of the order of an optical wavelength (indicating that  $\tau \gg \tau_c$ ) and that it was not the result of optical feedback from the device into the laser. To the best of our knowledge, laser phase-induced noise, with the particular spectral structure noted here, was not reported previously.

The output of the ac-coupled spectrum analyzer is related to its input  $v(t)$  by the Wiener-Kinchine theorem, namely: The autocovariance function of  $v(t)$ ,  $\langle [v(t+t') - \langle v(t) \rangle][v(t) - \langle v(t) \rangle] \rangle$  ( $\langle \rangle$  denotes an ensemble average) and the displayed spectrum  $S(f)$  are a Fourier-transform pair. Since the spectrum-analyzer input voltage is proportional to the output light intensity  $I(t)$ ,  $S(f)$  is related to the autocovariance function of  $I(t)$  by

$$\begin{aligned} \text{Cov}_I(t_1, t_2) &= \langle [I(t_1) - \langle I(t) \rangle][I(t_2) - \langle I \rangle] \rangle \\ &= P \int_{-\infty}^{+\infty} S(f) \exp[2\pi i(t_1 - t_2)f] df. \quad (1) \end{aligned}$$

The proportionality factor  $P$  depends on the detector responsivity and the amplifier gain as well as on the resolution setting of the spectrum analyzer. The observed spectrum of Fig. 3(a) can be approximated by  $a + b \sin^2(\pi f \tau)$  ( $a > 0, b > 0$ ), and by using Eq. (1) we may conclude that the intensity autocovariance function has at least the following components:  $(a + 0.5b)\delta(t_1 - t_2) - 0.25b[\delta(t_1 - t_2 - \tau) + \delta(t_1 - t_2 + \tau)]$ , where  $\delta(t)$  is the

Dirac delta function. Although the above approximation is crude in that it predicts infinite signal energy, it still indicates that the intensity autocovariance function is characterized by a positive narrow peak at the origin ( $t_1 - t_2 = 0$ ) and two negative narrow peaks at  $t_1 - t_2 = \pm\tau$ . We now proceed to show that this form of the autocovariance function can actually be predicted from a model that takes into consideration both the laser phase noise and the unitary nature of the directional coupler.

The input-output relationship of the directional coupler can be described by a  $2 \times 2$  complex transfer matrix,

$$\begin{pmatrix} E_3 \\ E_4 \end{pmatrix} = \begin{pmatrix} A & B \\ C & D \end{pmatrix} \begin{pmatrix} E_1 \\ E_2 \end{pmatrix}. \quad (2)$$

Here  $(E_1, E_2)$  and  $(E_3, E_4)$  are, respectively, the input and output complex amplitudes of the vector fields  $E_1, E_2, E_3$ , and  $E_4$ , which are assumed to have the same state of polarization. This last assumption is experimentally realized by winding a small length of the loop into a polarization controller,<sup>7,8</sup> which is then set to compensate for the loop birefringence so that the polarizations entering the coupler from the laser ( $E_1$ ) and the fiber loop ( $E_2$ ) are the same. (The coupler itself exhibits little dependence on the state of polarization of the input fields.<sup>9</sup>) Since backward reflections are negligibly small and loss in the coupler is usually less than 5%, the coupler matrix is approximately unitary; therefore  $|A|^2 + |B|^2 = |C|^2 + |D|^2 = 1$  and  $CA^* + DB^* = 0$  (the asterisk denotes complex conjugation).

The field amplitude at the output of the recirculating delay line ( $E_4$ ) is the sum of contributions from an infinite number of recirculations [Fig. 3(b)]:

$$\begin{aligned} E_4 &= C \exp[i\{\omega t + \phi(t)\}] + DA \sum_{n=1}^{n=\infty} B^{n-1} \exp(-na_0L) \\ &\quad \times \exp[i\{\omega(t - n\tau) + \phi(t - n\tau)\}], \quad (3) \end{aligned}$$

where  $\omega$  is the center optical frequency of the laser,  $\phi(t)$  is the laser phase noise, and we have assumed a laser emission of the form  $E_1 = \exp[i\{\omega t + \phi(t)\}]$  (at the input port of the coupler). Laser intensity noise has been neglected (see Fig. 2).  $\tau$  and  $L$  are, respectively, the loop delay and the loop length, and  $a_0$  is the fiber attenuation per unit length, which was of the order of several decibels/kilometer.<sup>8</sup> To explain the experimental observations, it is enough to consider only the first three terms ( $n \leq 2$ ) in Eq. (3) [see Fig. 3(b)] and to assume that  $a_0 = 0$ . The output voltage of the square-law detector is proportional to the incident light intensity, which has the following components:

$$\begin{aligned} I(t) &= |E_4|^2 = |C|^2 + |AD|^2 + |ABD|^2 \\ &\quad + 2|ACD| \cos[\phi(t) - \phi(t - \tau) + \omega\tau + \alpha] \\ &\quad + 2|A^2BD^2| \cos[\phi(t - \tau) \\ &\quad - \phi(t - 2\tau) + \omega\tau + \beta] \\ &\quad + 2|ABCD| \cos[\phi(t) - \phi(t - 2\tau) + 2\omega\tau + \gamma] \\ &= |C|^2 + |AD|^2 + |ABD|^2 \\ &\quad + S_1(t) + S_2(t) + S_3(t). \quad (4) \end{aligned}$$

$\alpha, \beta$ , and  $\gamma$  are, respectively, the arguments of the complex numbers  $C(DA)^*$ ,  $DA(DAB)^*$ , and

$DA(DAB)^*$ ; and  $S_1(t)$ ,  $S_2(t)$ , and  $S_3(t)$  are the three interference terms in  $I(t)$ .

Since the laser coherence time is  $\tau_c$ , it follows that, for two times  $t_a$  and  $t_b$ ,  $\phi(t_a)$  and  $\phi(t_b)$  are statistically independent unless  $|t_a - t_b| \lesssim \tau_c$ . We also assume that  $\tau \gg \tau_c$ , so that  $\langle I(t) \rangle = |C|^2 + |AD|^2 + |ABD|^2$  and  $\text{Cov}_I(t_1, t_2)$ , Eq. (1), can be readily constructed from Eq. (4):

$$\begin{aligned} \text{Cov}_I(t_1, t_2) = & 4 \langle [S_1(t_1)S_1(t_2) + S_2(t_1)S_2(t_2) \\ & + S_3(t_1)S_3(t_2)] \\ & + 4 \langle [S_1(t_1)S_2(t_2) + S_1(t_2)S_2(t_1)] \\ & + 4 \langle [S_1(t_1)S_3(t_2) + S_1(t_2)S_3(t_1) \\ & + S_2(t_1)S_3(t_2) + S_2(t_2)S_3(t_1)] \rangle. \end{aligned} \quad (5)$$

In evaluating the various terms in Eq. (5) we make frequent use of the fact that, when  $\tau \gg \tau_c$ ,<sup>10</sup>

$$\langle \cos[\phi(t_a) - \phi(t_b) + \phi(t_c) - \phi(t_d)] \rangle = 0 \quad (6)$$

unless either  $|t_a - t_b|$  and  $|t_c - t_d| \lesssim \tau_c$  or  $|t_a - t_d|$  and  $|t_b - t_c| \lesssim \tau_c$ . Using Eq. (6) in Eq. (5), we find that the terms in the first angle brackets in Eq. (5) generate a narrow positive peak around  $t_1 - t_2 = 0$ , the second angle brackets generate narrow peaks around  $t_1 - t_2 = \pm\tau$ , and the last angle brackets do not generate any significant contribution to  $\text{Cov}_I(t_1, t_2)$ . Hence

$$\text{Cov}_I(t_1, t_2) = \begin{cases} 2(|ACD|^2 + |A^2BD|^2 + |ABCD|^2) & t_1 - t_2 = 0 \\ 2|A^3BCD^3| \cos(\alpha - \beta) & t_1 - t_2 = \pm\tau \\ 0 & |t_1 - t_2| > \tau_c, |t_1 - t_2 \pm \tau| > \tau_c. \end{cases} \quad (7)$$

The widths of these three peaks are of the order of  $\tau_c$ . We now proceed to show that the peaks at  $t_1 - t_2 = \pm\tau$  are actually negative. Indeed, using the definitions of  $\alpha$  and  $\beta$  and the geometrical properties of complex numbers, we find that

$$\begin{aligned} \alpha - \beta &= \angle[C(DA)^*] - \angle[DA(DAB)^*] \\ &= \angle[A^*CD^*/|A|^2B^*|D|^2] \\ &= \angle[CA^*/DB^*] = \angle[-1] = \pi. \end{aligned} \quad (8)$$

The last equality results from the unitarity of the coupling matrix. Since  $\cos(\alpha - \beta) = -1$ , the intensity autocovariance function has the form of Fig. 4, and its Fourier transform will have lower values at  $f = m\tau$  (where the positive and negative spikes add destructively) than at  $f = (\frac{1}{2} + m)\tau$  (where they add constructively in the Fourier integral), as suggested by the experimental results ( $m$  is an integer, and our argument is valid whenever  $|f| \ll 1/\tau_c$ ).

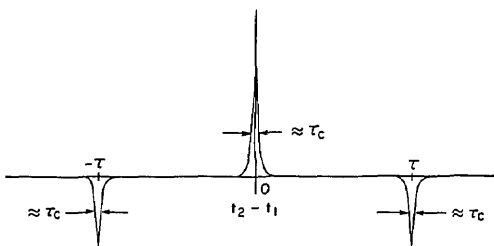


Fig. 4. Autocovariance function of the output light intensity generated by the first three terms in the expansion of Eq. (3). The power-coupling ratio was assumed to be 40%, i.e.,  $|B| = |C| \approx 0.63$  and  $|A| = |D| \approx 0.78$  in Eq. (2).

When all the higher-order terms of Eq. (3) are included, the same analysis shows that additional negative spikes will appear at all integer multiples of  $\tau$ , and their relative strengths will determine the shape of the basic period of the power spectrum.

The importance of the ratio  $\tau/\tau_c$  in the determination of the shape of the spectrum envelope as well as the detailed dependence of the spectrum on the coupling ratio and on the fiber birefringence and loss is under current investigation.

In summary, we have demonstrated the existence of phase-induced *spectrally structured* intensity noise in recirculating fiber delay lines. Noise with this particular form of power spectrum also appears in a bulk-optic recirculating interferometer with a beam splitter and mirrors that form an optical path that closes on itself. The magnitude of this phase-induced noise is important in assessing the ultimate dynamic range capabilities of optical signal processors with recirculating sections.

The authors wish to thank R. Bergh, J. E. Bowers, M. Chodorow, B. Culshaw, C. C. Cutler, J. W. Goodman, K. P. Jackson, G. S. Kino, L. F. Stokes, S. A. Newton, and H. J. Shaw for many helpful discussions. The couplers were fabricated by G. Kotler and J. Feth. The research described in this paper was supported by Litton Systems, Inc.

## References

1. M. Tur, J. W. Goodman, B. Moslehi, J. E. Bowers, and H. J. Shaw, "Fiber-optic signal processor with applications to matrix-vector multiplication and lattice filtering," *Opt. Lett.* **7**, 463-465 (1982).
2. J. E. Bowers, S. A. Newton, W. V. Sorin, and H. J. Shaw, "Filter response of single mode fiber recirculating delay lines," *Electron. Lett.* **18**, 110-111 (1982).
3. A. Dandridge and A. B. Tveten, "Phase noise of single-mode diode lasers in interferometer systems," *Appl. Phys. Lett.* **39**, 530-532 (1981).
4. Y. Yamamoto and T. Kimura, "Coherent optical fiber transmission systems," *IEEE J. Quantum Electron.* **QE-17**, 919-935 (1981).
5. J. A. Armstrong, "Theory of interferometric analysis of laser phase noise," *J. Opt. Soc. Am.* **56**, 1024-1031 (1966).
6. R. A. Bergh, G. Kotler, and H. J. Shaw, "Single-mode fibre optic directional coupler," *Electron. Lett.* **16**, 260-261 (1980).
7. H. C. Lefevre, "Single-mode fibre fractional wave devices and polarization controllers," *Electron. Lett.* **16**, 778-780 (1980).
8. L. F. Stokes, M. Chodorow, and H. J. Shaw, "All-single-mode fiber resonator," *Opt. Lett.* **7**, 288-290 (1982).
9. M. J. F. Dignonnet and H. J. Shaw, "Analysis of a tunable single mode fiber coupler," *IEEE J. Quantum Electron.* **QE-18**, 746-754 (1982).
10. K. Petermann and E. Weidel, "Semiconductor laser noise in an interferometer system," *J. Quantum Electron.* **QE-17**, 1251-1256 (1981).